Effect of Ce^{3+} and Ce^{4+} in Boro-Tellurite Based Glass on Optical and Structural Properties

N.A.M RUSNI[a], A. AZURAIDA[a*], A. NURAZLIN[a], L. HASNIMULYATI[b], W. Y. W. YUSOFF[a], NA ABDUL-MANAF[a]

[a] Physics Department, Centre for Defence Foundation Studies, Universiti Pertahanan Nasional Malaysia, 57000 Sungai Besi, Kuala Lumpur, Malaysia.

[b] Faculty of Applied Science, Universiti Teknologi MARA Cawangan Pahang, Kampus Jengka, 26400 Bandar Pusat Jengka, Pahan

Abstract

Enhancement of optical and structural properties of rare earth ions doped boro-tellurite glasses with high density modifiers become a new approach to achieve innovative optical glass devices. Motivated by this idea, three glass samples with the composition of $[(TeO_2)_{0.7}\ (B_2O_3)_{0.3}]_{0.75}\ (Bi_2O_3)_{0.25}$, $\{[(TeO_2)_{0.7}(B_2O_3)_{0.3}]_{0.75}(Bi_2O_3)_{0.25}\}_{0.99}\ (CeO_2)_{0.01}$ and $\{[(TeO_2)_{0.7}(B_2O_3)_{0.3}]_{0.75}(Bi_2O_3)_{0.25}\}_{0.98}\ (CeO_2)_{0.02}$ were successfully synthesized by conventional melt quenching method. A small amount of CeO_2 can enhance the glass density. The presence of Ce^{3+} and Ce^{4+} ions from CeO_2 assist in a compaction of the glass network which affects the result in density and molar volume. The absence of a sharp peak in X-ray Diffraction (XRD) spectra confirmed that all glass samples in this work are in an amorphous nature. Based on Fourier Transform Infrared Spectroscopy (FTIR) analysis, most of the glass samples consist of TeO_3, TeO_4, BO_3 and BO_4 structural units. The increase in refractive index value is also due to the presence of Ce^{3+} and Ce^{4+} ions in the glass network which leads to dense packing and is also affected by the increment in both electronic polarizability and optical basicity. The Urbach energy value continuously decreased after the addition of 0.02 mol CeO_2 signifies the reduction of defect concentration in the glass network. This in turn causes the reduced fragility nature of the glass and produces glass with high stability and connectivity.

Keywords: Boro-tellurite, bismuth oxide, cerium oxide, optical properties.

INTRODUCTION

The study of optical and structural properties is important to enable the proposed glass to be used in industrial application. It is important to choose material that has optimum structural and optical properties to maintain both transparency and structural strength of the material (1).

Recently, tellurite-based glass had attracted researchers' attention due to its physical and optical properties. High refractive index, low melting temperature and high-density energy are some of the interesting properties of tellurium dioxide glasses (2). As for optical properties, tellurium dioxide glass was found to have nonlinear susceptibilities in the order of 10 × than silicate based glass and thus offers an attractive opportunity for nonlinear applications (3). However, tellurium dioxide is a conditional glass former and cannot form glass on its own. Thus, it is important to choose the right modifier to enhance the glass properties.

It is known that the structure of pure TeO_2 glass mainly consists of TeO_4 trigonal bipyramid (tbp) structural units with a fraction of trigonal pyramids TeO_3 (tp) (4). When glass modifier was added to the tellurite glass network, the TeO_4 network breaks and change to TeO_3 units. The TeO_3 units were estimated to have lower polarizability than TeO_4 units. The ratio between TeO_4 and TeO_3 could be change to obtained desired specific measurement for the properties such as energy band gap, linear and non linear refractive index changes. In this study, boron oxide (B_2O_3) had been chosen as a glass modifier due to their high index of refraction, nonlinear optical properties and their high infrared transparency (~400 nm - 6 mm) along with their non-hygroscopic nature, tellurite glasses are good candidate for several optical and technological applications such as lasers, optical amplifiers, optical. Also, B_2O_3 has manufacturing benefits which are low in cost, high thermal stability and low melting point (5).

Nowadays, rare earth elements had been introduced to glass systems to enhance the properties of glass further. Cerium oxide (CeO_2) when added to glass composition, it acts as network formers. It had been found that when cerium oxide (CeO_2) was introduced to the borate glass, it reduces the number of non-bridging oxygens (NBOs) by converting BO_3 to BO_4 (6). Depending on the oxidizing and reducing conditions during glass fabrication, Cerium (Ce) ions can be in trivalent (Ce^{3+}) or tetravalent (Ce^{4+}) states. Achary *et al.*, (2017) (7) assigned that the oxidation state of Ce^{4+} ions are most stable in phosphate doped cerium glass. Demos *et al.* (2019) (8), found out that when Ce^{3+} doped fused silica samples was exposed to nanosecond ultraviolet laser pulses, Ce^{3+} exhibits strong absorption in the ultraviolet (UV) wavelength range and can be used as protective filters in high power lasers. Thus, cerium oxide was chosen as glass dopant due to its potential to be used for the fabrication of photonic devices.

Therefore, in this study, a new composition of bismuth-boro-tellurite glass doped with CeO_2 was synthesized and their structural as well as optical properties had been studied. This work is a continuation of our previous work (9) with the addition of cerium oxide.

METHODOLOGY

Glass Preparation: Three glasses with the chemical formula $[(TeO_2)_{0.7}\ (B_2O_3)_{0.3}]_{0.75}\ (Bi_2O_3)_{0.25}$, $\{[(TeO_2)_{0.7}(B_2O_3)_{0.3}]_{0.75}(Bi_2O_3)_{0.25}\}_{0.99}(CeO_2)_{0.01}$ and $\{[(TeO_2)_{0.7}(B_2O_3)_{0.3}]_{0.75}(Bi_2O_3)_{0.25}\}_{0.98}(CeO_2)_{0.02}$ have been prepared by using a melt quenching technique. First, chemicals in powder form from Assay, Alfa Aesar (tellurium (IV) dioxide TeO_2, boron oxide B_2O_3 and bismuth oxide Bi_2O_3) were mixed and ground thoroughly using an agate mortar for 20 minutes. The mixture was preheated at 400 °C for 30 minutes and then melted at 900 °C for 80 to 90 minutes. Subsequently, the molten glass was poured into a cylindrical stainless-steel mould, preheated at 400 °C and annealed at 400 °C for 90 to 120 minutes. When glass samples reached room temperature, they were cut and ground into powder form. Finally, the glass density, ρ, was determined using the Archimedes principle.

Glass Characterization:
X-Ray Diffraction (XRD) technique was used to identify the crystalline or amorphous nature of the glass sample. The fine powder of the glass sample was placed in a sample holder and compacted to form a plane surface. The sample holder was then transferred to the platform for measuring the XRD pattern by using Philips (PW 3040/60 MPD) X'pert High Pro X-ray Diffractometer in the 2θ range from 20° to 90° at room temperature.

The optical properties of glass samples were measured using a UV-VIS spectroscopy instrument known as Ultraviolet-Visible spectrophotometer. The basic parts of a spectrophotometer consist of a sample holder, a light source, a detector and a prism which is used to separate the different light wavelengths. The spectrophotometer is entirely software-driven and operates as a double-beam instrument, to split the light into two beams before it reaches the sample. Under this condition, one of the beams will pass through the sample while the other beam is used as the reference. To ensure successful measurement, the pellet of each glass sample was required to have a smooth surface on both sides and an average thickness of about 2 mm. The optical absorption spectra measured by UV-VIS spectrophotometer were taken in the wavelength range from 200 nm to 800 nm at room temperature.

RESULTS AND DISCUSSION

Physical and Structural Properties

The density of present glasses was successfully measured using Archimedes principle and listed in Table 1. It is observed that the density has increased from 5.85 gcm^{-3} to 5.92 gcm^{-3} when CeO_2 concentration has been added up to 0.02 % mol. Meanwhile, the molar volume had decreased from 36.95 cm^3mol^{-1} to 36.34 cm^3mol^{-1} when CeO_2 concentration increased to 0.02 % mol. It is postulated that the introduction of the high density of CeO_2 (7.65 gcm^{-3}) compared to TeO_2 (5.67 gcm^{-3}) and B_2O_3 (2.46 gcm^{-3}) may have increased the density of the glass system. The presence of cerium helps to decrease the bond length or interatomic spacing between the atoms which may be attributed to the increase in the stretching force constant of the bonds inside the glass network (10). The decrease in molar volume indicates that CeO_2 has a contracting effect (11). This means that the glass becomes more compact (12). According to Gedam *et al.*, (2013) (13), the density for $xCeO_2$-$15Li_2O$-$(85-x)B_2O_3$ glass system had increased from 2.076 gcm^{-3} to 2.140 gcm^{-3}. The high atomic weight of cerium ion from CeO_2 may change boron-to-boron ratio and result in conversion of BO_3 to BO_4^- unit. The increasing amount of BO_4^- unit is expected to cause an increment of glass density.

Table 1. Density (ρ) and molar volume (V_m), refractive index (n), molar refraction (R_m), molar polarizability (α_m), oxide ion polarizability (α_o^{2-}), optical band gap (E_{opt}) and urbach energy (ΔE), optical basicity (Λ), and metallization criterion, (M) for studied glass

Glass Composition	$[(TeO_2)_{0.7}(B_2O_3)_{0.3}]_{0.75}$ $(Bi_2O_3)_{0.25}$	$\{[(TeO_2)_{0.7}\ (B_2O_3)_{0.3}]_{0.75}$ $(Bi_2O_3)_{0.25}\}_{0.99}(CeO_2)_{0.01}$	$\{[(TeO_2)_{0.7}\ (B_2O_3)_{0.3}]_{0.75}$ $(Bi_2O_3)_{0.25}\}_{0.98}$ $(CeO_2)_{0.02}$
% mol of CeO_2	0	0.01	0.02
Glass Name	25BiBTe	25BiBTe-1Ce	25BiBTe-2Ce
ρ (gcm^{-3})	5.85	5.91	5.92
V_m ($cm^3\ mol^{-1}$)	36.95	36.48	36.34
n	1.955	2.090	2.098
R_m	18.829	18.899	19.062

α_m (Å^3)	8.947	8.939	8.957
α_o^{2-} (Å^3)	5.897	5.911	5.985
$E_{opt,direct}$ (eV)	2.210	2.26	2.37
$E_{opt,indirect}$ (eV)	1.56	1.82	1.92
ΔE (eV)	0.472	0.281	0.264
Λ	1.028	1.089	1.091
M	0.360	0.369	0.365

In this work, the average boron–boron separation, $\langle d_{B\text{-}B} \rangle$ has been calculated to confirm the compaction of glass structure after addition of glass modifier/dopant. The results are presented in Table 1. The average boron-boron separation $\langle d_{B\text{-}B} \rangle$ is calculated using the equation:

$$\langle d_{B-B} \rangle = \left(\frac{V_m^B}{N_A} \right)^{1/3} \quad (6)$$

where N_A is Avogadro's number (6.0228×10^{23} gmol^{-1}) and V_m^B is the volume which corresponds to the volume that contains one mole of boron within the given structure. This volume, V_m^B are determined using the following relation:

$$V_m^B = \frac{V_m}{2(1 - x_B)} \quad (7)$$

where x_B is the molar fraction of boron oxide, B_2O_3 and V_m is the molar volume of glass.

The average boron-boron separation $\langle d_{B\text{-}B} \rangle$ is calculated to give more insight into the modification of the glass network due to the presence of CeO_2. The boron atoms are the central atoms with negatively charged tetrahedral - $BO_{4/2}$ units (14). Since V_m^B depends on cation species. Therefore, the calculated values of average boron-boron separation $\langle d_{B\text{-}B} \rangle$ are decreased with the increase in the CeO_2 contents in the glass system as shown in Table 1. Thus, the incorporation of V_m^B on the expense of B_2O_3 leads to a substantial expansion of the glass structural network confirming the obtained density and molar volume values (15). Furthermore, the calculated values of boron molar volume V_m^B illustrate that with increasing CeO_2 contents together at the expense of boron oxide, the V_m^B is increased since V_m^B depends on cation species. Therefore, with the increase in the CeO_2 contents, the decrement in the average boron-boron separation may be obtained. Thus, the incorporation of CeO_2 at the expense of B_2O_3 leads to a substantial non-densification of the glass structural network which approves the obtained density and molar volume values. The increase in the bond length or inter-atomic spacing between the atoms may also be attributed to a decrease in the stretching force constants of the bonds inside the glass network (13).

XRD analysis

X-ray diffraction pattern for studied glasses showed no sharp peak that represented amorphous nature as shown in Figure 1 and 2. Similar pattern of the XRD graph also shown in multicomposition borotellurite glasses which was reported by Hasnimulyati *et al.* (2016) (16) and Aboud *et al.*(17). The absence of a sharp peak indicates that there is no long-range order in atomic arrangements which confirmed that all glass samples in this work are amorphous. Furthermore, a broad bump is shown indicates the wide range peak of glasses due to the variation of inter-atomic distance. However, when Bi_2O_3 was added at the maximum concentration, the intensity of the broad halo at $2\theta \cong 24 - 30^{\circ}$ began to rise and eventually became a little peak. The atomic rearrangements in the glass structure that result in proper alignment causes these modifications. According to Kindrat *et al.* (2016) (18), the atomic rearrangement is almost like a crystalline molecule. In the XRD spectra of the examined glasses, Kaur *et al.* (2016) (19), revealed the presence of a minor hump that was attributed to heat loss and the formation of nucleation sites. Periodic arrangements of certain atoms during the quenching process atoms led to the formation of nucleation sites.

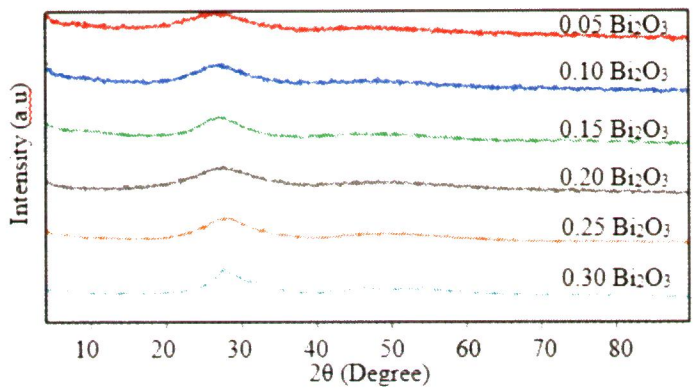

Figure 1 XRD pattern of $[(TeO_2)_{0.7}\ (B_2O_3)_{0.3}]_{0.75}\ (Bi_2O_3)_{0.25}$ glass before and after irradiated with different doses of gamma ray

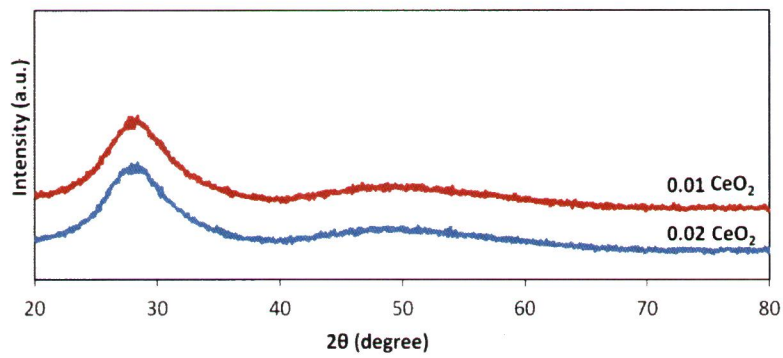

Figure 2 XRD pattern of [(TeO2)0.7 (B2O3)0.3]0.75 (BaO)0.25 glass before and after irradiated with different doses of gamma ray

Optical Properties

The optical absorption spectra for all glass have been measured in the range of 220 – 800 nm at room temperature. The result is provided in Figure 3.

A graph between $(\alpha h\omega)^{1/2}$ and $(h\omega)$ s called Tauc's plot. For fundamental absorption edge in lower incident photon energy $(h\omega)$ between 10^2 - 10^4 cm^{-1}, absorption coefficient $\alpha(\omega)$ follows Urbach law given by:

$$\alpha(\omega) = B\ exp\left(\frac{h\omega}{\Delta E}\right) \qquad (8)$$

where B is a constant and ΔE is the Urbach's energy. The Urbach energy values are calculated from the slopes of linear regions of the plots $\ln\alpha(\omega)$ vs $\hbar\omega$. The wavelength values corresponding to the absorption edge, where the intensity reaches the maximum value in optical absorption spectra are taken as cut-off wavelengths, $\lambda_{cut\text{-}off}$.

From Figure 3, it can be observed that the absorption edge is more prominent in the visible region. This is because the addition of CeO_2 causes the absorption edge to gradually shift towards the shorter wavelength and become more sharper gradually. El-Mallawany, (2002) (20) reported that the sharp absorption edge observed when CeO_2 was introduced into TeO_2 - P_2O_5 glass is caused by forbidden transition involving the 4f levels. These 4f orbits are very effectively shielded from interaction with external fields of the hosts by $5s^2$ and $5p^6$ shells. Meanwhile, the shift of absorption edge towards the shorter wavelength due to the decreasing number of non-bridging oxygen in the glass system. Bahadur *et al.*, (2010) (21) has also stated that the shifted of absorption edge depends on the chemical composition used in preparing glass. Also, it is related to the electron donating power which is influenced by the constituent of the glass and the electronegativity of the cations such as Ba^{2+}, Na^{+}, Ce^{3+}, Ce^{4+}, etc.

The observed shift in the absorption edge might be due to the formation of the hole centres by the reaction of Ce^{3+} + HC→Ce^{4+} and the ceric ions prevent the formation of induced centres by the reaction of Ce^{4+}+ EC→Ce^{3+}. HC is the hole centre captured by the cations and EC is the electron centre captured by the anions (22).

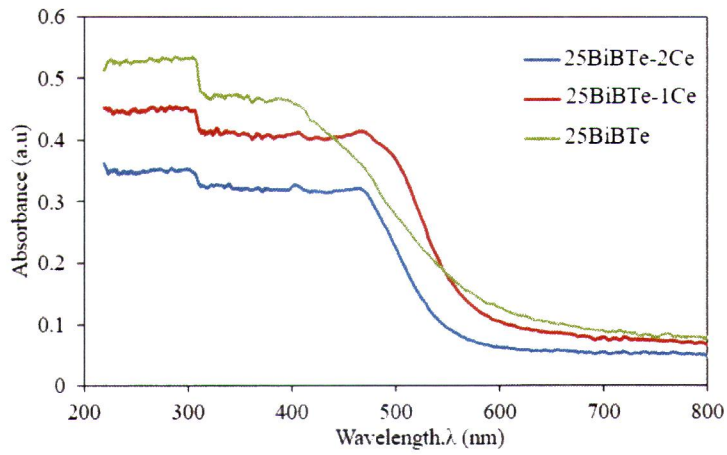

Figure 3 Optical absorption for all glasses

The optical band gap, E_{opt} for all glasses have been predicted from Figures 4 and 5. The E_{opt} value for direct transition is increased by about ~8% and for indirect transition is also increased by about ~20% as stated in Table 1. The increment of E_{opt} is maybe due to the increase of bridging oxygen atoms in the glass system. According to Khafagy *et al.*, 2008 (23), bridging oxygens that hold electron tightly causes the electron to need more energy in order to jump from the valence into the conduction band, leading to the rise in the optical band gap. Besides that, the increase in E_{opt} may also be caused by the rise in the connectivity of the glass network. As the atoms are more connected to one another, the valence and conduction band will widen their gap and thus increase the optical band gap (24).

Another reason for the increasing value of the optical band gap in this series glass is that the cerium ion was larger in size compared to boron and tellurium ion. Therefore, the distance between the top of the valence band and the conduction band becomes bigger. Abdel-Kader *et al.*, (1993) (25) reported the values of E_{opt} for TeO_2 - P_2O_5 glass doped CeO_2 is 3.04 eV and for glass doped La_2O_3 the value is 3.03 eV. The higher value of E_{opt} in CeO_2 could be due to the larger atomic number of cerium (58) compared to Lanthanum (57). This factor may be attributed to the compactness of the glass, which increases E_{opt}. The increasing pattern in the optical band gap was also found in tellurite-based glass doped Nd_2O_3 and Er_2O_3 (26). The increase of the optical band gap could be due to the substitution of other components in glasses with Nd_2O_3 and Er_2O_3. Therefore, increasing Nd_2O_3 and Er_2O_3 will increase the optical band gap because it facilitates polaron hopping and conductivity increases by hopping. Consequently, there was an increase in E_{opt} resulting from the energy level of Nd_2O_3 and Er_2O_3. In addition, the increase in E_{opt} by further addition of CeO_2 content is could be due to decreasing number of NBO and it was agreeable with decreasing value shown in Urbach energy. The Urbach energy, ΔE values which are calculated from taking the reciprocal of the slope of the linear portion of the graph Ln(α) against $\hbar\omega$ in Figure 6 were found to decrease with the increase of CeO_2 concentration. The ΔE value has decreased from 0.508 to 0.281 after the addition of 0.01 mol fraction CeO_2 in the glass system. The value decreased again to 0.264 when the CeO_2 amount was increased to 0.02 mol fraction. The decreasing value signified the reduction of defect concentration in the glass network. This in turn might have causes the fragility nature of the glass to decrease and produced glass with high stability and connectivity (27). Similar results have been reported in boro-tellurite based glass doped rare-earth (La_2O_3) (28). Both direct and indirect optical band gap were increased from 2.20 to 3.90 eV and 2.20 to 3.43 eV, respectively. Meanwhile, the Urbach energy value was observed to decrease from 0.47 to 0.33 eV as the mol fraction of La_2O_3 increased up to 0.05. When the amount of the lanthanum ion increases, the number of BO_3 units decreases and the bridging oxygen increases. The small value of Urbach energy could be due to the decrease of disorderness and fragility in the glass structure.

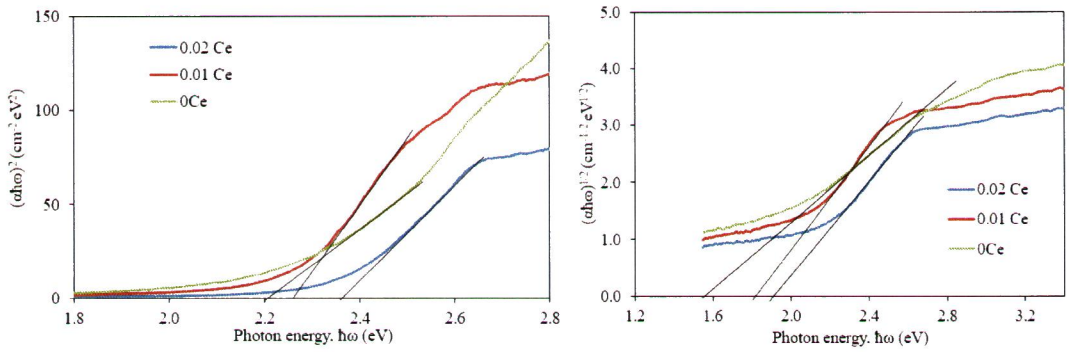

Figure 4 (a) Plot of $(\alpha\hbar\omega)^2$ against $\hbar\omega$ for all glasses, (b) Plot of $(\alpha\hbar\omega)^{1/2}$ against $\hbar\omega$ for studied glasses

The refractive index of all glasses is obtained from Equation (1). As the glass becomes denser, the velocity of light that passes through the sample will become slower and finally result in the elevation of the refractive index. This is in good agreement with previous work by Saddeek *et al.*, 2010 (29).

The refractive index for studied glasses increases with the increase of CeO_2 content. The value has increased from 2.090 to 2.098, which attributes to the increase in cerium ion and the increasing glass density. Refractive index can be defined as the ratio of the velocity of light in a vacuum to the velocity of light in a specified medium. As expected, the refractive index is higher in a denser material compared to a lower density material because the velocity of light is slower in high density material. The addition of CeO_2 in glass system leads to the formation of TeO_3 asymmetric polyhedron with one short, three elongated Te-O bonds and TeO_3 trigonal pyramids with non-bridging oxygen. The high polarizability of non-bridging oxygen than the bridging oxygen causes high refractive index glasses. In addition, the presence of rare earth ions (Ce^{3+} and Ce^{4+}) in glass network leads to the formation of dense packing. The refractive index is known to have a directly proportional relationship to dense packing (26). Besides that, the increased value of molar polarizability as shown in Table 1 is also the main contributing factor to the increment of the refractive index. The high polarizability of cerium ion and non-bridging oxygen ion present in the glass network causes the increment of its molar polarizability, oxide ion polarizability, molar refraction and refractive index.

Umar *et al.*, (2017) (30) reported the optical energy band gap of tellurite-boro-silicate glass doped Er_2O_3 was increased as the concentration of Er_2O_3 concentration was increased up to 0.05 mol%. On the other hand, the refractive index showed a decreasing pattern from 2.521 to 2.452 with an increasing amount of Er_2O_3. This observation may be attributed to the replacement of a Te^{4+} with Er^{3+} ions, which has higher polarizability. The increase in the molar refraction, R_m value in their work from 22.237 to 22.440 may be due to the increase in the polarizability value.

The ability of oxide glass to provide negative charges in the glass network is known as optical basicity (Λ). The oxygen atoms behaves as Lewis bases due to their ability to donate a portion of their negative charge to cations which can be dependent by the number of Non-Bridging Oxygen (NBOs) in the glass system (31,32). Based on Table 1, the optical basicity (Λ) value after irradiated for $[(TeO_2)_{0.7}(B_2O_3)_{0.3}]_{0.75}(Bi_2O_3)_{0.25}$ are 1.028. When CeO_2 was added to the glass composition, the Λ increases to 1.089 and 1.091 for $\{[(TeO_2)_{0.7}(B_2O_3)_{0.3}]_{0.75}(Bi_2O_3)_{0.25}\}_{0.99}(CeO_2)_{0.01}$ and $\{[(TeO_2)_{0.7}(B_2O_3)_{0.3}]_{0.75}(Bi_2O_3)_{0.25}\}_{0.99}(CeO_2)_{0.02}$ respectively. It can be inferred that the ionic nature of the examined glasses increases while covalent nature decreases when CeO_2 was added to the glass composition(31,32). Furthermore, Masai *et al* (2021) (33) found that an oxidation reaction from Ce^{3+} to Ce^{4+} preferentially occurs in their glass sample assumed that a higher valence state is suitable for a glass matrix with a higher Λ value. Also, it is inferred that the higher molar polarizability (α_m) and oxide ion polarizability (α_o^{2-}) of CeO_2 doped glass might also be responsible for higher Λ value (34).

Metallization criterion (M) in Table 1 refers to the behavior of the glass samples which is either the glass exhibits metallic or non-metallic behavior. The value of M depends in the value of molar refractivity (R_m) and molar volume (V_m) based on the equation as follows (31,35): -

$$M = 1 - \left(\frac{R_m}{V_m}\right) \quad (9)$$

Based on the ration of $\frac{R_m}{V_m}$, metallic and non-metallic behavior can be determined. If the ratio are greater than 1, the nature of the material is metals and if the ratio are lower than 1, the nature of the material is non-metal (36–38). When $\frac{R_m}{V_m} = 1$, refractive index would become limitless and metallization of covalent solid material occurs where electrons are able to travel freely inside the material. Observing the result in Table 1, for glass samples $[(TeO_2)_{0.7}(B_2O_3)_{0.3}]_{0.75}(Bi_2O_3)_{0.25}$, $\{[(TeO_2)_{0.7}(B_2O_3)_{0.3}]_{0.75}(Bi_2O_3)_{0.25}\}_{0.99}(CeO_2)_{0.01}$ and $\{[(TeO_2)_{0.7}(B_2O_3)_{0.3}]_{0.75}(Bi_2O_3)_{0.25}\}_{0.98}(CeO_2)_{0.02}$ the value for M is 0.360, 0.369 and 0.365 respectively. Since the M is lower than 1, all glass samples exhibit non-metallic also known as insulating behaviour. It is also found that M increase slightly as CeO_2 added to the glass compositions. This is due to decreasing width of both valence and conduction band, which results in increasing optical band gap. The decrease of valence band width might be due to the production of more bridging-oxygens (BOs) in the glass network. Since the bonding orbital of BOs has lower energies compared to non-bridging oxygens (NBOs), it causes the maximum valence band to shift to lower energies, making it narrow. This result correlates with the study done by Hasnimulyati (2017) (37).

CONCLUSION

Three glass samples $[(TeO_2)_{0.7}(B_2O_3)_{0.3}]_{0.75}(Bi_2O_3)_{0.25}$, $\{[(TeO_2)_{0.7}(B_2O_3)_{0.3}]_{0.75}(Bi_2O_3)_{0.25}\}_{0.99}(CeO_2)_{0.01}$ and $\{[(TeO_2)_{0.7}(B_2O_3)_{0.3}]_{0.75}(Bi_2O_3)_{0.25}\}_{0.98}(CeO_2)_{0.02}$ were successfully synthesized by conventional melt quenching method. Glass sample with 2% CeO_2 has the highest density as high density CeO_2 increase the density of the glass system. Contradict, molar volume decreases as CeO_2 increases due contracting effect of CeO_2 which increase the compactness of the glass sample. The compactness of the glass sample was confirmed with average boron-boron separation $\langle d_{B\text{-}B} \rangle$ decreases with increasing CeO_2 contents in the glass system. Furthermore, the absence of a sharp peak in XRD spectra have confirmed that all glass samples in this work are amorphous. As for the optical absorption spectra, the absorption edge is more prominent in the visible region because the addition of CeO_2 causes the absorption edge to gradually shift towards the shorter wavelength and become more sharper gradually. Moreover, the E_{opt} value for direct transition and indirect transition increases due to the increase of bridging oxygen atoms in the glass system causing the valence and conduction band will widen their gap. The increase in E_{opt} by further addition of CeO_2 content was agreeable with decreasing value shown in ΔE. The ΔE values was found to decrease with the increase of CeO_2 concentration. The decreasing value signified the reduction of defect concentration in the glass network. Furthermore, the refractive index for studied glasses increases with the increase of CeO_2 because Ce^{3+} and Ce^{4+} in glass network leads to the formation of dense packing. Also, when CeO_2 was added to the glass composition, the Λ increases because ionic nature of the examined glasses increases while covalent nature decreases. As for metallic behaviour, since all glass samples' M value is lower than 1, all glass samples exhibit non-metallic also known as insulating behaviour.

Acknowledgements

The authors appreciate the financial support from Universiti Pertahanan Nasional Malaysia with Short Term Grant UPNM/2022/GPJP/SG/3.

References

1. Orosun MM, Usikalu MR, Oyewumi KJ. Radiological hazards assessment of laterite mining field in

Ilorin, North-central Nigeria. Int J Radiat Res. 2020;18(4):895–906.

2. Bürger H, Vogel W, Kozhukharov V, Marinov M. Phase equilibrium, glass-forming, properties and structure of glasses in the TeO2-B2O3 system. J Mater Sci [Internet]. 1984 [cited 2022 Dec 27];19(2):403–12. Available from: https://link.springer.com/article/10.1007/BF02403226

3. Manning S, Ebendorff-heidepriem H, Monro TM. Ternary tellurite glasses for the fabrication of nonlinear optical fibres. 2012;2(2):305–8.

4. Elkholy H, Othman H, Hager I, Ibrahim M, de Ligny D. Thermal and optical properties of binary magnesium tellurite glasses and their link to the glass structure. J Alloys Compd [Internet]. 2020;823:153781. Available from: https://doi.org/10.1016/j.jallcom.2020.153781

5. Dwaikat N, Sayyed MI, Mhareb MHA, Dong M, Alajerami YSM, Alrammah I, et al. Durability, optical and radiation shielding properties for new series of boro-tellurite glass. Int J Light Electron Opt [Internet]. 2021; Available from: https://doi.org/10.1016/j.ijleo.2021.167667

6. El-Damrawi G, Gharghar F, Ramadan R. More Insight on Structure of New Binary Cerium Borate Glasses. New J Glas Ceram. 2018;08(01):12–21.

7. Achary SN, Bevara S, Tyagi AK. Recent progress on synthesis and structural aspects of rare-earth phosphates. Coord Chem Rev. 2017 Jun 1;340:266–97.

8. Demos SG, Ehrmann PR, Qiu SR, Schaffers KI, Suratwala TI. Dynamics of defects in Ce^3+ doped silica affecting its performance as protective filter in ultraviolet high-power lasers. Opt Express. 2014;22(23):28798.

9. Azuraida A, Halimah MK, Sidek AA, Azurahanim CAC, Iskandar SM, Ishak M, et al. Comparative studies of bismuth and barium boro-tellurite glass system: Structural and optical properties. Chalcogenide Lett. 2015;12(10):497–503.

10. Vani P, Vinitha G, Sayyed MI, AlShammari MM, Manikandan N. Effect of rare earth dopants on the radiation shielding properties of barium tellurite glasses. Nucl Eng Technol [Internet]. 2021;53(12):4106–13. Available from: https://doi.org/10.1016/j.net.2021.06.009

11. Hasnimulyati L, Halimah MK, Zakaria A, Halim SA, Ishak M. A comparative study of the experimental and the theoretical elastic data of Tm3+ doped zinc borotellurite glass. Mater Chem Phys [Internet]. 2017;192:228–34. Available from: http://dx.doi.org/10.1016/j.matchemphys.2017.01.086

12. Kaur P, Singh GP, Kaur S, Singh DP. Modifier role of cerium in lithium aluminium borate glasses. J Mol Struct [Internet]. 2012;1020(December 2017):83–7. Available from: http://dx.doi.org/10.1016/j.molstruc.2012.03.053

13. Gedam RS, Ramteke DD. Influence of CeO2 addition on the electrical and optical properties of lithium borate glasses. J Phys Chem Solids. 2013;74(10):1399–402.

14. Pal Singh G, Kaur P, Kaur S, Singh DP. Gamma ray effect on the covalent behaviour of the CeO2-BaO-B2O3 glasses. Phys B Condens Matter [Internet]. 2014;450(December 2017):106–10. Available from: http://dx.doi.org/10.1016/j.physb.2014.05.017

15. Ibrahim S, Gomaa MM, Darwish H. Influence of Fe2O3 on the physical, structural and electrical properties of sodium lead borate glasses. J Adv Ceram. 2014;3(2):155–64.

16. Halimah MK, Hasnimulyati L, Zakaria A, Halim SA, Ishak M, Azuraida A, et al. Influence of gamma radiation on the structural and optical properties of thulium-doped glass. Mater Sci Eng B Solid-State Mater Adv Technol [Internet]. 2017;226(May):158–63. Available from: http://dx.doi.org/10.1016/j.mseb.2017.09.010

17. Aboud H, Aldhuhaibat MJR, Alajermi Y. Gamma radiation shielding traits of B2O3–Bi2O3–CdO–BaO. Radiat Phys Chem [Internet]. 2022 [cited 2022 Jun 27]; Available from: https://doi.org/10.1016/j.radphyschem.2021.109836

18. Kindrat II, Padlyak B V., Mahlik S, Kukliński B, Kulyk YO. Spectroscopic properties of the Ce-doped borate glasses. Opt Mater (Amst). 2016;59:20–7.

19. Kaur K, Singh KJ, Anand V. Structural Properties of Bi2O3-B2O3-SiO2-Na2O Glasses for Gamma Ray Shielding Applications. Radiat Phys Chem. 2016;120:63–72.

20. El-Mallawany. Tellurite Glasses Handbook: Physical Properties and Data. Washington DC: CRC Press; 2002.

21. Bahadur A, Dwivedi Y, Rai SB. Spectroscopic study of Er:Sm doped barium fluorotellurite glass. Spectrochim Acta - Part A Mol Biomol Spectrosc. 2010;77(1):101–6.

22. Bulus I, Hussin R, Ghoshal SK, Tamuri AR, Jupri SA. Enhanced elastic and optical attributes of boro-telluro-dolomite glasses: Role of CeO2 doping. Ceram Int [Internet]. 2019;45(15):18648–58. Available from: https://doi.org/10.1016/j.ceramint.2019.06.089

23. Khafagy AH, El-Adawy AA, Higazy AA, El-Rabaie S, Eid AS. Studies of some mechanical and optical properties of: (70 − x)TeO2 + 15B2O3 + 15P2O5 + xLi2O glasses. J Non Cryst Solids. 2008 Jun 1;354(27):3152–8.

24. Saffarini G, Schmitt H, Shanak H, Nowoczin J, Müller J. Optical band gap in relation to the average coordination number in Ge—S—Bi thin films. basic solid state Phys [Internet]. 2003 Sep 1 [cited 2022 Dec 29];239(1):251–6. Available from: https://onlinelibrary.wiley.com/doi/full/10.1002/pssb.200301821

25. Abdel-Kader A, El-Mallawany R, Elkholy MM. Network structure of tellurite phosphate glasses: Optical absorption and infrared spectra. J Appl Phys [Internet]. 1998 Jun 4 [cited 2022 Dec 29];73(1):71. Available from: https://aip.scitation.org/doi/abs/10.1063/1.354064

26. El-Mallawany R, Abdalla MD, Ahmed IA. New tellurite glass: Optical properties. Mater Chem Phys. 2008 Jun 15;109(2–3):291–6.

27. Gayathri Pavani P, Sadhana K, Chandra Mouli V. Optical, physical and structural studies of boro-zinc tellurite glasses. Phys B Condens Matter. 2011 Mar 15;406(6–7):1242–7.

28. Halimah MK, Faznny MF, Azlan MN, Sidek HAA. Optical basicity and electronic polarizability of zinc borotellurite glass doped La3+ ions. Results Phys. 2017 Jan 1;7:581–9.

29. Saddeek YB, Aly KA, Bashier SA. Optical study of lead borosilicate glasses. Phys B Condens Matter [Internet]. 2010;405(10):2407–12. Available from: http://dx.doi.org/10.1016/j.physb.2010.02.055

30. Umar SA, Halimah MK, Chan KT, Latif AA. Polarizability, optical basicity and electric susceptibility of Er3 + doped silicate borotellurite glasses. J Non Cryst Solids [Internet]. 2017 Sep 1 [cited 2022 Dec 29];471:101–9. Available from: http://scienceon.kisti.re.kr/srch/selectPORSrchArticle.do?cn=NART78229422

31. Divina R, Marimuthu K, Mahmoud KA, Sayyed MI. Physical and structural effect of modifiers on dysprosium ions incorporated boro-tellurite glasses for radiation shielding purposes. Ceram Int [Internet]. 2020;46(11):17929–37. Available from: https://doi.org/10.1016/j.ceramint.2020.04.102

32. Mariyappan M, Marimuthu K, Sayyed MI, Dong MG, Kara U. Effect Bi2O3 on the physical, structural and radiation shielding properties of Er3+ ions doped bismuth sodium fluoroborate glasses. J Non Cryst Solids [Internet]. 2018;499(May):75–85. Available from: https://doi.org/10.1016/j.jnoncrysol.2018.07.025

33. Masai H, Kimura H, Akatsuka M, Kato T, Yanagida T. Correlation between luminescence of cerium and chemical compositions in lithium silicate-based glasses. Opt Mater (Amst) [Internet]. 2021;121(June):111631. Available from: https://doi.org/10.1016/j.optmat.2021.111631

34. Azuraida A. Structural, Optical and Shielding Properties of Bi2O3/BaO-B2O3-TeO2 Doped CeO2 Glass System. Universiti Putra Malaysia. 2018.

35. El-mallawany R. Tellurite Glass Smart. Cham Switzerland: Springer International Publishing AG; 2018.

36. Teresa PE, Naseer KA, Piotrowski T, Marimuthu K, Aloraini DA, Almuqrin AH, et al. Optical properties and radiation shielding studies of europium doped modifier reliant multi former glasses. Optik (Stuttg) [Internet]. 2021;247(July). Available from: https://doi.org/10.1016/j.ijleo.2021.168005

37. Hasnimulyati L. Effect of Gamma Radiation on Elastic and Optical Properties of Tm2O3/CeO2-Doped Zinc Borotellurite Glass System. Universiti Putra Malaysia; 2017.

38. Asyikin AS, Shamimi AA, Nazrin SN, Halimah MK, Boukhris I. The effect of manganese (IV) oxide doping on the optical and elastic properties of calcium borate glass derived from waste chicken eggshell. Opt Mater (Amst) [Internet]. 2021;121(July). Available from: https://doi.org/10.1016/j.optmat.2021.111540